

COOPERATIVE TRACKING ALGORITHM OF MULTIPLE UAVS USING PSO FOR AERIAL SURVEILLANCE

Dayeon Yoon[1], Jaeyeon Ka[1], Dongjin Lee*[1], Zihao Wang[2] & KC Wong[2]

[1]Hanseo University, 46 Hanseo 1-ro, Haemi-myeon, Seosan-si, Chungcheongnam-do, Republic of Korea, 31962
[2]The University of Sydney, Camperdown, NSW, Australia, 2006

Abstract

Unauthorized aerial vehicles pose significant security risks to restricted airspace surrounding airports and military installations, requiring surveillance systems capable of real-time localization and continuous tracking. However, conventional ground-based surveillance systems may suffer from shadowed regions caused by installation constraints, limited sensor coverage, and line-of-sight occlusions from terrain and buildings. This paper proposes a particle swarm optimization (PSO)-based cooperative waypoint generation algorithm for multiple aerial surveillance UAVs to support persistent tracking of unauthorized aerial vehicles. Using the updated target-state estimate, the proposed algorithm generates cooperative waypoints that improve observation geometry while considering trajectory continuity and flight-energy consumption. The objective function includes bearing-angle, elevation-angle, trajectory-continuity, and flight-energy terms, and practical constraints such as target–UAV tracking range, inter-UAV safety distance, velocity limit, and yaw-rate limit are incorporated. The proposed algorithm was evaluated in a MATLAB/ROS2–Gazebo simulation environment using three aerial surveillance UAVs under straight and circular target trajectory scenarios. Compared with a Fisher Information Matrix (FIM)-based waypoint generation method, the proposed method reduced the 2D localization RMSE by approximately 23.5% in the straight trajectory scenario and 22.2% in the circular trajectory scenario, while maintaining safe inter-UAV separation. These results validate the effectiveness of the proposed PSO-based cooperative tracking algorithm in improving target localization accuracy and supporting stable multi-UAV tracking under operational constraints.

Keywords: Unauthorized Aerial Vehicles, Multi-UAV Cooperative Tracking, Waypoint Planning, Particle Swarm Optimization (PSO)

1. Introduction

The rapid expansion of commercial drone applications has increased the risk of unauthorized aerial vehicle incursions around critical infrastructure, including airports, military bases, and nuclear power plants [1]. Since these vehicles often fly at low altitude, have small physical size, and exhibit high maneuverability, airspace surveillance systems must provide real-time localization and persistent tracking. However, ground-based surveillance systems using radar, radio-frequency (RF) sensors, and electro-optical (EO) cameras can suffer from shadowed regions caused by sensor installation geometry, limited coverage, line-of-sight (LOS) occlusions, and environmental conditions. These regions may cause temporary measurement loss, increased target-state uncertainty, and possible track loss, as illustrated in Figure 1.

Aerial surveillance UAVs can mitigate these limitations by providing additional viewpoints in regions that are difficult to observe from the ground. Previous studies have investigated ground–aerial surveillance sensor networks, cooperative unmanned aerial vehicle (UAV)–unmanned ground vehicle (UGV) target localization, and ground–aerial collaborative detection and path planning [2],[3],[4]. In particular, multiple UAVs can improve target observability by forming favorable observation geometry, which requires waypoint generation methods for maintaining effective viewing angles around the target.

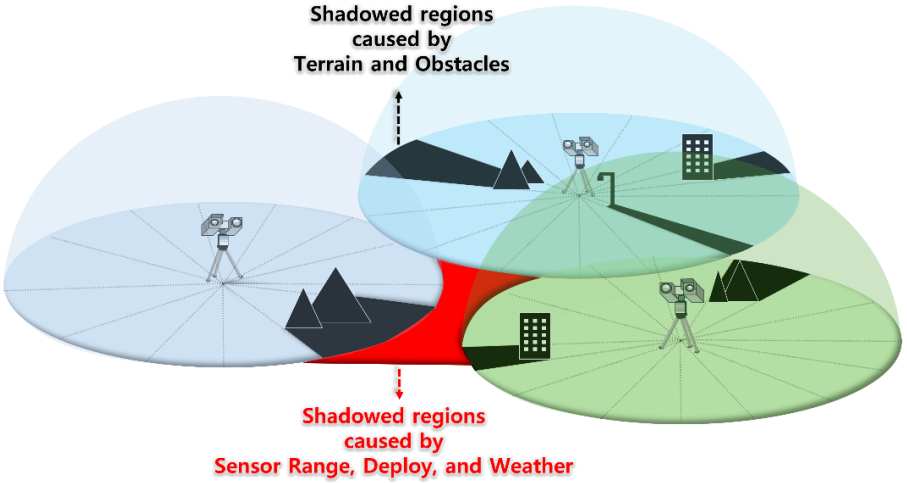


Figure 1 – Example of shadowed regions in ground-based surveillance.

Information-based path planning methods using the Fisher Information Matrix (FIM) or the Cramér–Rao Lower Bound (CRLB) have been widely studied for optimizing observation geometry [5],[6],[7]. However, FIM-based approaches can be affected by linearization errors in nonlinear measurement models and sensitivity to measurement noise and initial estimation errors. To address these limitations, this study directly guides observation geometry based on the bearing-angle distribution among multiple aerial surveillance UAVs.

Cooperative waypoint generation for multiple UAVs is a nonlinear constrained optimization problem because localization performance, flight feasibility, collision avoidance, and trajectory continuity are coupled. Therefore, this paper proposes a PSO-based cooperative waypoint generation algorithm for persistent tracking of unauthorized aerial vehicles in shadowed regions caused by LOS occlusions. The proposed algorithm generates feasible waypoints using the latest target-state estimate while considering localization performance, flight-energy consumption, trajectory continuity, and operational constraints.

2. System Overview

The proposed cooperative ground–aerial surveillance system consists of ground surveillance equipment, a ground control station, and N aerial surveillance UAVs, as shown in Figure 2. The ground surveillance equipment performs wide-area surveillance and provides initial detection data for an unauthorized aerial vehicle. The ground control station receives the target information from the ground surveillance equipment, as well as target observations and UAV state information from the aerial surveillance UAVs. Based on these measurements, the target-state estimate is updated at each tracking cycle.

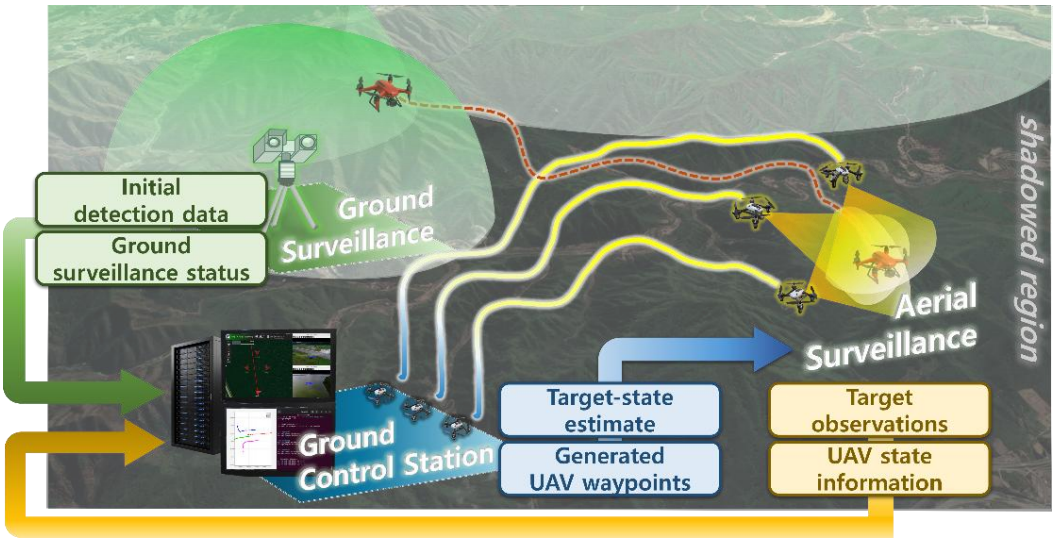


Figure 2 – Overall framework of the proposed PSO-based cooperative tracking system.

At tracking cycle k, the estimated position vector of the unauthorized aerial vehicle, denoted by $\widehat{\boldsymbol{P}}_t(k)$, is represented in geodetic coordinates as

$$\widehat{\boldsymbol{P}}_t(k) = [\hat{\phi}_t(k) \quad \hat{\lambda}_t(k) \quad \hat{h}_t(k)] \tag{1}$$

where $\hat{\phi}_t(k)$, $\hat{\lambda}_t(k)$, and $\hat{h}_t(k)$ denote the latitude, longitude, and altitude of the estimated target position, respectively. Using this estimate and the current UAV states, the waypoint generator computes the cooperative waypoint set as

$$\boldsymbol{W}(k) = \{\boldsymbol{w}_1(k), \boldsymbol{w}_2(k), \cdots, \boldsymbol{w}_N(k)\} \tag{2}$$

where $\boldsymbol{w}_i(k) = \left[\phi_i^{wp}(k) \quad \lambda_i^{wp}(k) \quad h_i^{wp}(k)\right]$ denotes the latitude, longitude, and altitude of the waypoint assigned to the i-th aerial surveillance UAV, and N is the number of UAVs. The generated waypoints are transmitted to the corresponding UAVs, and each UAV tracks its assigned waypoint while continuously observing the target with an electro-optical sensor.

This process is repeated whenever a new target-state estimate is obtained. Through this closed-loop structure, the proposed system continuously updates the cooperative waypoint set according to target motion and observation conditions.

3. Method

3.1 Cooperative Tracking Problem Formulation

The cooperative waypoint generation module uses the updated target-state estimate and the current UAV states to generate a feasible waypoint set for the aerial surveillance UAVs. The objective is to maintain favorable observation geometry around the target while satisfying practical flight and safety constraints.

The cooperative waypoint generation problem is formulated as a constrained optimization problem. The total cost function is defined as

$$F_{\text{total}} = F_{\text{object}} + \rho C_{\text{total}} \tag{3}$$

where F_{object} represents the objective cost related to tracking performance and path quality, C_{total} is the total constraint violation penalty, and ρ is the penalty coefficient.

The objective cost and constraint penalty are defined as

$$F_{\text{object}} = \omega_1 F_{\text{bearing}} + \omega_2 F_{\text{elevation}} + \omega_3 F_{\text{position}} + \omega_4 F_{\text{energy}} \tag{4}$$

$$C_{\text{total}} = C_{\text{tracker}} + C_{\text{collision}} + C_{\text{velocity}} + C_{\text{yawrate}} \tag{5}$$

The deviation-related objective terms are formulated as squared residuals to penalize positive and negative deviations symmetrically and to assign larger penalties to larger deviations. The constraint terms are formulated as normalized non-negative squared violation penalties, which become zero when the corresponding constraints are satisfied. Since the constraint penalties are normalized, ρ was selected to prioritize feasible waypoint generation over objective-cost minimization. The weighting factors were empirically selected and kept fixed throughout all simulation scenarios. The weighting factors and penalty coefficient are summarized in Table 1.

Table 1 – Weighting factors for the objective and constraint penalty terms.

Parameter	Value	Description
ω_1	2.0	Weight of bearing angle cost
ω_2	0.3	Weight of elevation angle cost
ω_3	1.0	Weight of trajectory continuity cost
ω_4	2.0	Weight of flight energy cost
ρ	10^3	Penalty coefficient

3.1.1 Objective Function

The objective function improves cooperative observation geometry while maintaining smooth and energy-efficient UAV trajectories. All distance-based terms are evaluated in a local metric coordinate frame. The bearing-angle and elevation-angle geometries are illustrated in Figure 3.

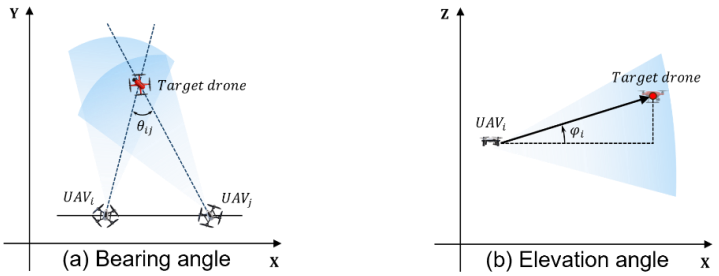


Figure 3 – Localization geometry for the bearing angle and elevation angle cost terms: (a) bearing angle and (b) elevation angle.

The bearing cost encourages the aerial surveillance UAVs to form a favorable angular distribution around the target:

$$F_{\text{bearing}} = \sum_{i=1}^{N-1} \sum_{j=i+1}^{N} \left(\frac{\theta_{ij}(k) - \theta_d}{\theta_d} \right)^2 \tag{6}$$

$$\theta_d = \begin{cases} \dfrac{\pi}{2}, & N = 2 \\ \dfrac{2\pi}{N}, & N \geq 3 \end{cases} \tag{7}$$

where $\theta_{ij}(k)$ is the bearing angle between UAV i and UAV j with respect to the estimated target position as illustrated in Figure 3(a), and θ_d is the desired bearing angle for cooperative localization.

The elevation cost penalizes excessively steep viewing geometry:

$$F_{\text{elevation}} = \sum_{i=1}^{N} \left[\max\left(0, \frac{|\varphi_i(k)| - \varphi_{\max}}{\varphi_{\max}} \right) \right]^2 \tag{8}$$

where φ_i is the elevation angle from UAV i to the target as illustrated in Figure 3(b), and $\varphi_{\max}$ is the maximum allowable absolute elevation angle and is set to 30 deg. The absolute value is used to avoid restricting the UAVs to only one side of the target in the vertical direction.

The trajectory-continuity cost is defined to reduce abrupt waypoint changes between consecutive tracking cycles.

$$F_{\text{position}} = \sum_{i=1}^{N} \|\boldsymbol{w}_i(k) - \boldsymbol{w}_i(k-1)\|^2 \tag{9}$$

This term suppresses discontinuous waypoint transitions caused by the stochastic nature of PSO and helps generate smooth UAV trajectories over time.

The energy consumption of UAV i is estimated using the rotary-wing UAV energy model in [11], which accounts for hovering, cruising, and turning motions. The flight-energy cost is defined as

$$F_{\text{energy}} = \sum_{i=1}^{N} E_i(k) \tag{10}$$

where $E_i(k)$ is the estimated energy consumption of UAV i.

3.1.2 Constraints

The generated waypoints must satisfy four operational constraints: target–UAV tracking range, inter-UAV safety distance, velocity limit, and yaw-rate limit. Each constraint is evaluated using a normalized non-negative squared violation penalty. For an upper-bound constraint, the violation is calculated as $\max(0, x - x_{\max})/x_{\max}$, whereas for a lower-bound constraint, it is calculated as $\max(0, x_{\min} - x)/x_{\min}$. Therefore, each penalty term becomes zero when the corresponding constraint is satisfied and increases quadratically as the degree of violation increases.

First, the target–UAV tracking range constraint is considered to maintain continuous target observation. To maintain continuous detection and tracking, each aerial surveillance UAV must remain within the effective tracking range:

$$d_{\text{tracker,min}} \le d_{i,\text{target}}(\text{k}) \le d_{\text{tracker,max}}, \quad \forall i \in \{1, \cdots, N\} \tag{11}$$

where $d_{i,\text{target}}(\text{k})$ denotes distance between the generated waypoint of UAV i and the estimated target position, $d_{\text{tracker,min}}$ and $d_{\text{tracker,max}}$ denote the minimum and maximum allowable target–UAV distances, respectively. In this study, $d_{\text{tracker,min}}$ is set to 60 m and $d_{\text{tracker,max}}$ is set to 120 m. The target–UAV tracking range penalty is defined as

$$C_{\text{tracker}} = \sum_{i=1}^{N} \left[\frac{\max(0, d_{i,\text{target}}(k) - d_{\text{tracker,max}})}{d_{\text{tracker,max}}} \right]^2 + \sum_{i=1}^{N} \left[\frac{\max(0, d_{\text{tracker,min}} - d_{i,\text{target}}(k))}{d_{\text{tracker,min}}} \right]^2 \tag{12}$$

Second, the inter-UAV safety distance constraint is imposed to prevent collisions between aerial surveillance UAVs. To ensure safe multi-UAV operation, the inter-UAV distance must be greater than the minimum safety distance:

$$d_{\text{collision}} \le d_{i,j}(\text{k}), \quad \forall i < j \tag{13}$$

where $d_{i,j}(\text{k})$ denotes distance between the generated waypoints of UAV i and UAV j, $d_{\text{collision}}$ denotes the minimum allowable safety distance between two UAVs. In this study, $d_{\text{collision}}$ is set to 50 m. The inter-UAV collision-avoidance penalty is defined as

$$C_{\text{collision}} = \sum_{i=1}^{N} \sum_{j=i+1}^{N} \left[\frac{\max(0, d_{\text{collision}} - d_{ij}(k))}{d_{\text{collision}}} \right]^2 \tag{14}$$

Third, the velocity constraint ensures that each generated waypoint is reachable within the UAV speed limit during one tracking cycle. The required transition speed of UAV i is defined using the distance between its current position and the generated waypoint:

$$v_i(k) \le v_{\max}, \quad \forall i \in \{1, \cdots, N\} \tag{15}$$

where $v_{\max}$ is the maximum allowable UAV speed. In this study, $v_{\max}$ is set to 15 m/s. The velocity-limit penalty is defined as

$$C_{\text{velocity}} = \sum_{i=1}^{N} \left[\frac{\max(0, v_i(k) - v_{\max})}{v_{\max}} \right]^2 \tag{16}$$

Finally, the yaw-rate constraint limits rapid heading changes required to maintain target observation. The heading change of UAV i between consecutive tracking cycles must satisfy

$$|\Delta\psi_i(k)| \le \omega_{\max}\Delta t, \quad \forall i \in \{1, \cdots, N\} \tag{17}$$

where $\Delta\psi_i(k)$ is the heading change of UAV i between consecutive tracking cycles, and $\omega_{\max}$ is the maximum yaw rate. In this study, $\omega_{\max}$ is set to 30 deg/s. The yaw-rate penalty is defined as

$$C_{\text{yawrate}} = \sum_{i=1}^{N} \left[\frac{\max(0, |\Delta\psi_i(k)| - \omega_{\max}\Delta t)}{\omega_{\max}\Delta t} \right]^2 \tag{18}$$

3.2 PSO-based Cooperative Waypoint Generation

PSO is adopted to search for cooperative waypoint solutions in the continuous waypoint space. To improve convergence, an initial feasible waypoint set is obtained using the MATLAB fmincon solver, and the PSO particles are initialized around this solution within the predefined search bounds. The overall procedure is shown in Figure 4.

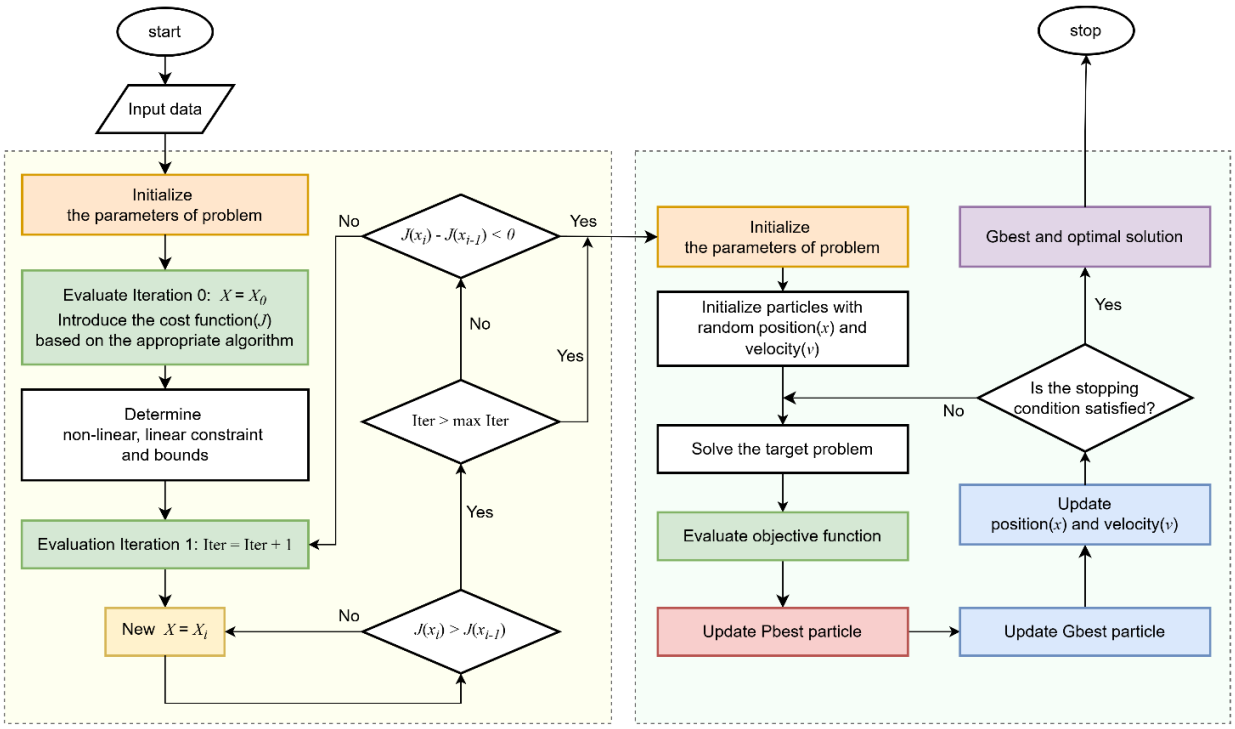


Figure 4 – Flowchart of the proposed PSO-based cooperative waypoint generation algorithm.

Each particle updates its velocity and position based on its personal best solution and the global best solution:

$$v_j^{r+1} = \omega v_j^r + c_1 r_1 \left(\mathrm{p}_{j,\mathrm{best}} - z_j^r\right) + c_2 r_2 \left(\mathrm{g}_{\mathrm{best}} - z_j^r\right) \tag{19}$$

$$z_j^{r+1} = z_j^r + v_j^{r+1} \tag{20}$$

where z_j^r and v_j^r denote the position and velocity of particle j at iteration r, respectively. $\mathrm{p}_{j,\mathrm{best}}$ and $\mathrm{g}_{\mathrm{best}}$ are the personal best and global best positions, respectively. The parameters ω, c_1, and c_2 are the inertia weight, cognitive coefficient, and social coefficient, while r_1 and r_2 are random values between 0 and 1.

After convergence, g_{best} is selected as the optimal cooperative waypoint vector. The main PSO parameters are summarized in Table 2. Since three aerial surveillance UAVs are used and each waypoint consists of latitude, longitude, and altitude, the dimension of each PSO particle is set to 9.

Table 2 – PSO parameters.

Parameter	Value	Parameter	Value
c_1	0.2	r_1	0~1
c_2	2.0	r_2	0~1
ω	0.1~1.1	Population	80
Upper bound	[36.6650, 126.3520, 67.5]	Max Iterations	1800
Lower bound	[36.6590, 126.3410, 47.5]	Dimension	9

3.3 Waypoint Tracking Guidance

After the optimal cooperative waypoints are generated in Section 3.2, each aerial surveillance UAV tracks its assigned waypoint using a waypoint-based guidance law. The guidance command consists of a velocity command for waypoint tracking and a heading command for maintaining target observation.

The velocity command is generated to move each UAV toward its assigned waypoint:

$$\boldsymbol{v}_{i,cmd} = K_p\left(\boldsymbol{w}_i(k) - \boldsymbol{P}_i^{\mathrm{UAV}}\right) \tag{21}$$

where $v_{i,cmd}$ is the velocity command of the i-th UAV, K_p is the velocity proportional gain, $\boldsymbol{w}_i(k)$ is the waypoint assigned to the i-th UAV, and $\boldsymbol{P}_i^{\mathrm{UAV}}(k)$ is the current position of the UAV.

To maintain target observation, the heading command is generated to keep the UAV oriented toward the estimated target position:

$$\psi_{i,cmd} = \mathrm{atan2}\left(R_E\left(\hat{\lambda}_t - \lambda_i\right)\cos\phi_i\,, R_E\left(\hat{\phi}_t - \phi_i\right)\right) \tag{22}$$

where $\psi_{i,cmd}$ is the heading command of the i-th UAV, R_E is the Earth radius, $(\hat{\phi}_t,\ \hat{\lambda}_t)$ denotes the latitude and longitude of the estimated target position, and $(\phi_i\,,\ \lambda_i)$ denotes the latitude and longitude of the i-th UAV. Through this guidance structure, each UAV moves toward its assigned cooperative waypoint while maintaining its sensor direction toward the target.

4. Simulation and Evaluation

4.1 Simulation Environment

A MATLAB/ROS2–Gazebo simulation environment was developed to validate the proposed cooperative waypoint generation algorithm, as shown in Figure 5. The simulation includes a standard VTOL model as the unauthorized aerial vehicle and multiple PX4-based X-500 multicopters as aerial surveillance UAVs. At each tracking cycle, the estimated target state and UAV states are provided to the PSO-based waypoint generator, and the generated waypoints are transmitted to the UAVs through the ROS2 interface for PX4-based waypoint tracking.

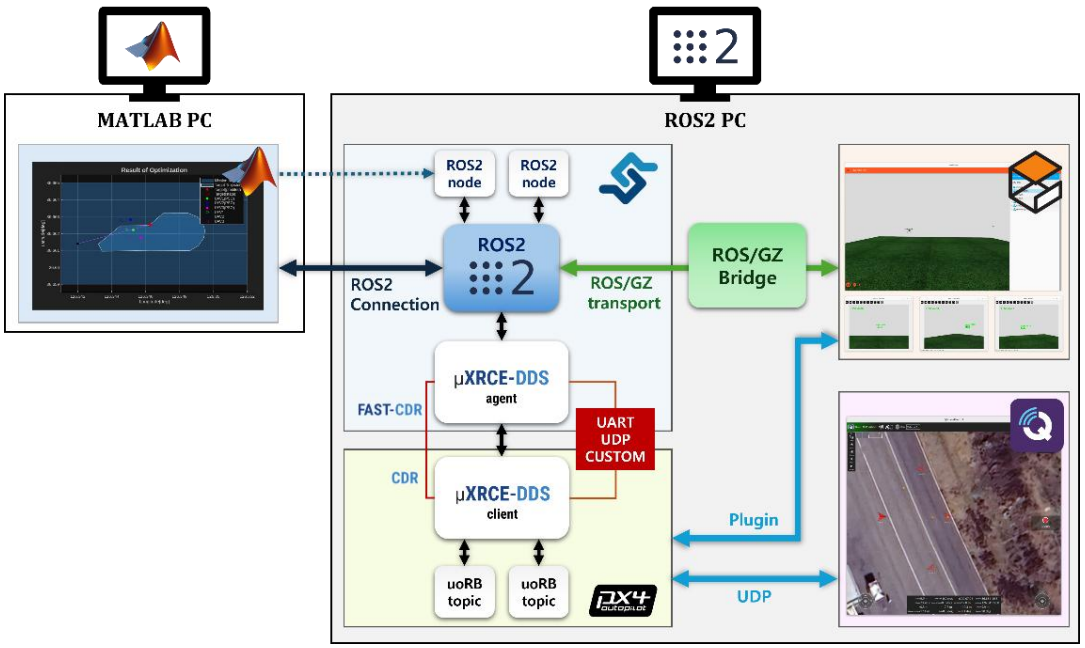


Figure 5 – MATLAB/ROS2–Gazebo simulation environment.

The main simulation conditions are summarized in Table 3. Two target-tracking scenarios were considered: a straight trajectory and a circular trajectory.

Table 3 – Common simulation conditions for the target-tracking scenarios.

Object	Parameter	Unit	Value
Unauthorized aerial vehicle	Max velocity	m/s	10
Aerial surveillance UAVs	Max velocity	m/s	15
	Max yaw rate	deg/s	30
	Camera FOV	deg	50

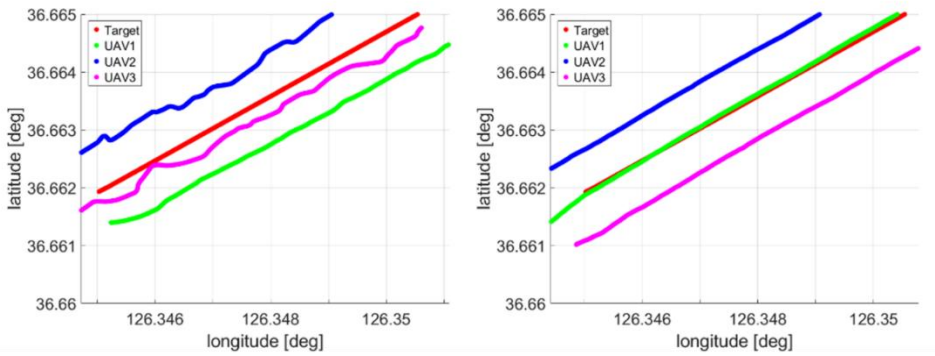
To evaluate the proposed method, a Fisher Information Matrix (FIM)-based waypoint generation method using A-optimality and D-optimality was used as a baseline. Performance was evaluated in terms of localization accuracy, UAV trajectory continuity, and inter-UAV separation.

$$F_{\text{total}}^{\text{baseline}} = F_{\text{A-optimality}} + F_{\text{D-optimality}} \tag{23}$$

where $F_{\text{A-optimality}}$ and $F_{\text{D-optimality}}$ denote the A-optimality and D-optimality terms used in the FIM-based baseline method, respectively.

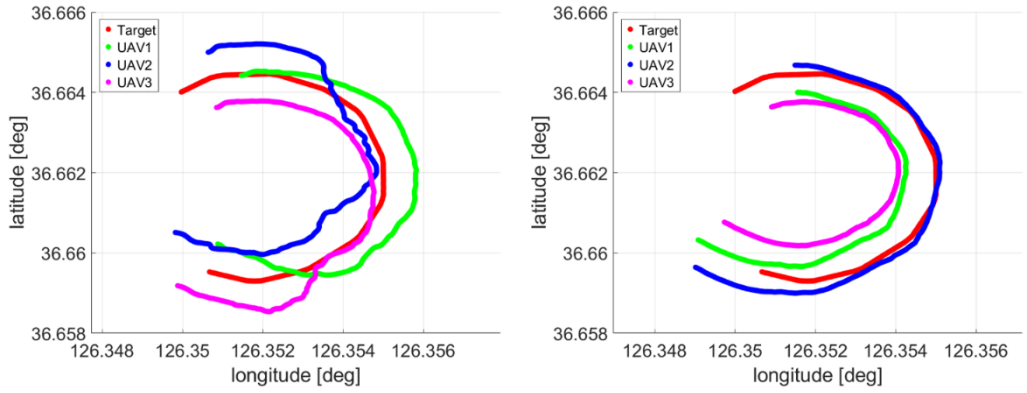
4.2 Evaluation

Both methods successfully tracked the target in both scenarios, as shown in Figures 6 and 7. Compared with the FIM-based baseline, the proposed method generated smoother UAV trajectories while maintaining cooperative observation geometry around the target. All UAV pairs also maintained distances above the minimum inter-UAV safety distance throughout the simulation, confirming that the collision-avoidance constraint was satisfied.



(a) Trajectory of FIM-based baseline (b) Trajectory of proposed method

Figure 6 – Simulation results of waypoint generation and tracking in the straight trajectory scenario: (a) FIM-based baseline and (b) proposed method.



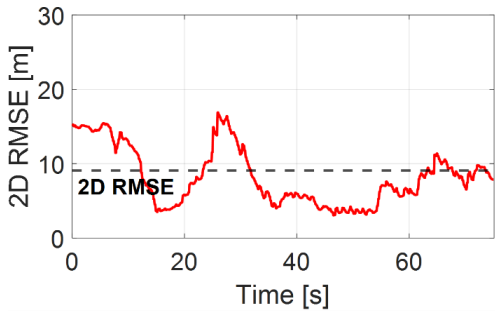
(a) Trajectory of FIM-based baseline (b) Trajectory of proposed method

Figure 7 – Simulation results of waypoint generation and tracking in the circular trajectory scenario: (a) FIM-based baseline and (b) proposed method.

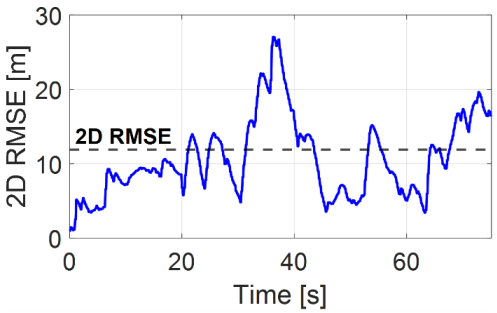
The localization error results for the straight and circular trajectory scenarios are shown in Figures 8 and 9, respectively, and summarized in Table 4. In the straight trajectory scenario, the proposed method reduced the 2D RMSE from 11.877 m to 9.084 m, corresponding to an improvement of approximately 23.5%. In the circular trajectory scenario, the 2D RMSE was reduced from 15.167 m to 11.807 m, corresponding to an improvement of approximately 22.2%. The 50th and 90th percentile errors were also reduced in both scenarios, indicating that the proposed method improves the overall target-position estimation accuracy.

Table 4 – Localization error comparison in the straight and circular trajectory scenarios.

Scenario	Method	2D RMSE [m]	50^{th} error [m]	90^{th} error [m]
Straight	Proposed	9.084	7.340	14.719
Straight	FIM-based	11.877	9.363	17.928
Circular	Proposed	11.807	9.330	19.101
Circular	FIM-based	15.167	10.238	27.257

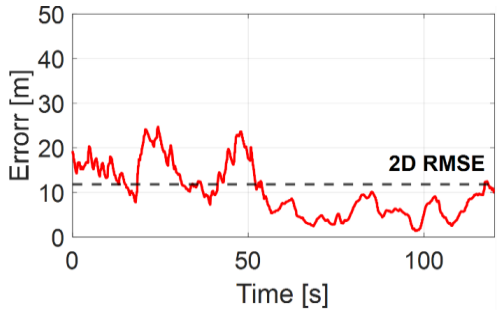


(a) 2D RMSE of position estimation (proposed method)

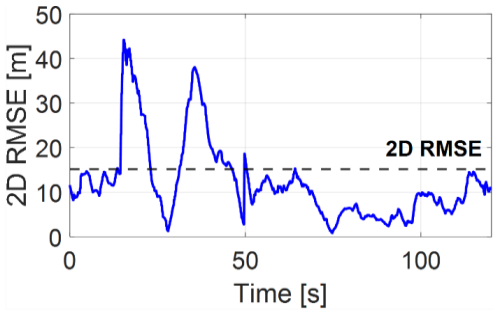


(b) 2D RMSE of position estimation (FIM-based method)

Figure 8 – Localization error comparison in the straight trajectory scenario: (a) proposed method and (b) FIM-based baseline.



(a) 2D RMSE of position estimation (proposed method)



(b) 2D RMSE of position estimation (FIM-based method)

Figure 9 – Localization error comparison in the circular trajectory scenario: (a) proposed method and (b) FIM-based baseline.

5. Conclusion and Future Work

In this study, a PSO-based cooperative waypoint generation algorithm was proposed for persistent tracking of unauthorized aerial vehicles in shadowed regions caused by line-of-sight occlusions. The proposed method uses aerial surveillance UAVs to maintain target observability when ground-based observations are degraded and generates cooperative waypoints based on the updated target-state estimate. The waypoint generator considers bearing-angle geometry, elevation-angle geometry, trajectory continuity, and flight-energy consumption while satisfying practical constraints, including target–UAV range, inter-UAV safety distance, velocity limit, and yaw-rate limit.

The proposed method was evaluated in a MATLAB/ROS2–Gazebo simulation environment using

straight and circular target trajectory scenarios. Compared with the FIM-based baseline method, the proposed method reduced the 2D localization RMSE from 11.877 m to 9.084 m in the straight trajectory scenario and from 15.167 m to 11.807 m in the circular trajectory scenario, corresponding to improvements of approximately 23.5% and 22.2%, respectively. The simulation results validate that the proposed method improves target localization accuracy while maintaining safe inter-UAV separation during cooperative tracking.

Future work will extend the proposed framework to environments with multiple ground surveillance systems. In particular, ground–aerial data fusion will be investigated so that observations from multiple ground sensors and aerial surveillance UAVs can be jointly used for target-state estimation. This extension is expected to improve tracking robustness under partial occlusions, intermittent measurement availability, and complex target maneuvers.

6. Contact Author Email Address

Dongjin Lee*[1], djlee@hanseo.ac.kr

7. Copyright Statement

The authors confirm that they, and/or their company or organization, hold copyright on all of the original material included in this paper. The authors also confirm that they have obtained permission, from the copyright holder of any third party material included in this paper, to publish it as part of their paper. The authors confirm that they give permission, or have obtained permission from the copyright holder of this paper, for the publication and distribution of this paper as part of the ICAS proceedings or as individual off-prints from the proceedings.

References

[1] Famili A, Stavrou A, Wang H, Park J-M and Gerdes R. Securing your airspace: detection of drones trespassing protected areas. *Sensors*, Vol. 24, No. 7, Paper 2028, 2024.

[2] Deng X, Liu Y, Zhu C and Zhang H. Air–Ground surveillance sensor network based on edge computing for target tracking. *Computer Communications*, Vol. 166, pp 254–261, 2021.

[3] Liu D, Bao W, Zhu X, Fei B, Xiao Z and Men T. Vision-aware air-ground cooperative target localization for UAV and UGV. *Aerospace Science and Technology*, Vol. 124, Paper 107525, 2022.

[4] Ma T, Lu P, Deng F and Geng K. Air–Ground collaborative multi-target detection task assignment and path planning optimization. *Drones*, Vol. 8, No. 3, Paper 110, 2024.

[5] Hou W, Zhang X, Li J and Liu Z. Optimal geometry and motion coordination for multisensor target tracking with bearings-only measurements. *Sensors*, Vol. 23, No. 14, Paper 6408, 2023.

[6] Dogancay K and Hmam H. UAV path optimization for angle-only self-localization and target tracking based on the Bayesian Fisher information matrix. *Sensors*, Vol. 24, No. 10, Paper 3120, 2024.

[7] Wang W, Bai P, Li H and Liang X. Optimal configuration and path planning for UAV swarms using a novel localization approach. *Applied Sciences*, Vol. 8, No. 6, Paper 1001, 2018.

[8] Roberge V, Tarbouchi M and Labonté G. Comparison of parallel genetic algorithm and particle swarm optimization for real-time UAV path planning. *IEEE Transactions on Industrial Informatics*, Vol. 9, No. 1, pp 132–141, 2013.

[9] de Oliveira N S M M, Moreira E M and Rosa P F F. Particle swarm optimization algorithm implementation for multiple drones control in continuous task simulation. *Proc 2019 Latin American Robotics Symposium*, 2019 Brazilian Symposium on Robotics and 2019 Workshop on Robotics in Education, Rio Grande, Brazil, pp 363–368, 2019.

[10] Meng Q, Chen K and Qu Q. PPSwarm: multi-UAV path planning based on hybrid PSO in complex scenarios. *Drones*, Vol. 8, No. 5, Paper 192, 2024.

[11] Choi Y, Choi Y, Briceno S and Mavris D N. Energy-constrained multi-UAV coverage path planning for an aerial imagery mission using column generation. *Journal of Intelligent & Robotic Systems*, Vol. 97, No. 1, pp 125–139, 2020.